Published in final edited form as:
Immunity. 2008 October 17; 29(4): 589–601. doi:10.1016/j.immuni.2008.08.011.

Spatiotemporal regulation of T cell co-stimulation by TCR-CD28 microclusters through PKCθ translocation

Tadashi Yokosuka[*], **Wakana Kobayashi**[*], **Kumiko Sakata-Sogawa**[§], **Akiko Hashimoto-Tane**[*], **Michel L. Dustin**[#,¶], **Makio Tokunaga**[§,=,‡], and **Takashi Saito**[*,¶]

[*] Laboratory for Cell Signaling, RIKEN Center for Allergy and Immunology, 1-7-22 Suehiro-cho, Tsurumi-ku, Yokohama 230-0045, Japan

[§] Single-Molecule Immunoimaging, RIKEN Center for Allergy and Immunology, 1-7-22 Suehiro-cho, Tsurumi-ku, Yokohama 230-0045, Japan

[=] Structural Biology Center, National Institute of Genetics, The Graduate University for Advanced Studies, Mishima, Shizuoka 411-8540, Japan

[‡] Department of Genetics, The Graduate University for Advanced Studies, Mishima, Shizuoka 411-8540, Japan

[#] Program in Molecular Pathogenesis, Skirball Institute of Biomolecular Medicine and Department of Pathology, New York University School of Medicine, 540 First Avenue, New York, NY 10016, USA

[¶] WPI Immunology Frontier Research Center, Suita, Osaka 565-0081, Japan

Summary

T cell activation is mediated by microclusters (MCs) containing TCRs, kinases, and adaptors. Although TCR-MCs translocate to form a central supramolecular activation cluster (c-SMAC) of immunological synapse between T cells and antigen-presenting cells (APCs), the role of MC translocation in T cell signaling remains unclear. Here, we found that the accumulation of MCs in c-SMAC was important for T cell co-stimulation. Using planar bilayer system, co-stimulatory receptor CD28 was initially recruited coordinately with TCR to MCs and its signals was mediated through the assembly with PKCθ. Their co-localization and assembly is correlated withco-stimulatory function. The accumulation of MCs at c-SMAC was accompanied by segregation of CD28 from TCRs and both CD28 and PKCθ translocated to a spatially unique sub-zone of c-SMAC. Thus, co-stimulation is mediated by generating a novel co-stimulatory compartment in c-SMAC via the dynamic regulation of MC translocation.

Introduction

T cells require two distinct signals for their activation and differentiation; an antigen (Ag)-recognition signal transmitted through TCRs upon recognition of Ag—major histocompatibility complex (MHCp) on APCs and a co-stimulatory signal through co-stimulatory receptors upon binding to their ligands expressed on APCs. Co-stimulatory signals are essential particularly for the induction of full activation of T cells leading to cytokine production, proliferation, survival, and functional differentiation. In order to induce a proper activation of T cells through co-stimulation, co-stimulatory receptors and their signals should

Correspondence: Takashi Saito, Laboratory for Cell Signaling, RIKEN Center for Allergy and Immunology, 1-7-22 Suehiro-cho, Tsurumi-ku, Yokohama 230-0045, Tel +81-45-503-7037, Fax +81-45-503-7038, saito@rcai.riken.jp.

be provided in appropriate strength and timing by dynamic and quantitative regulation. Modulation of co-stimulatory signals for T cell activation have been attempted in the clinical setting including modulation of autoimmune diseases, such as rheumatoid arthritis and psoriasis, prevention of graft versus host disease in transplantation, effective vaccinations, and improving anti-tumor immunity (Riley and June, 2005; Salomon and Bluestone, 2001).

Among known co-stimulatory receptors, CD28 plays a predominant role in co-stimulation by binding its ligands, CD80 and CD86 (Acuto and Michel, 2003; Chambers et al., 2001; Rudd and Schneider, 2003; Sharpe and Freeman, 2002). CD28 is constitutively expressed on both naïve and effector T cells. CD86 is constitutively expressed at low levels on most professional APCs and is rapidly upregulated after activation, whereas CD80 is inducibly expressed more lately. Studies of genetically modified mice lacking CD28 or CD80/CD86 have confirmed that CD28 signals play roles in the augmentation of a variety of T cell functions, includingcell-cycle progression, anti-apoptotic function, cytokine production, T helper polarization, cytotoxic T cell differentiation, and maturation of humoral immunity. In addition to these direct functions, CD28-mediated signals are indicated to upregulate other co-stimulatory, cytokine, chemokine receptors, consequently inducing secondary co-stimulatory responses. Although the downstream signals of CD28 have been extensively analyzed for more than a decade, the precise mechanisms are not clearly understood. Many molecules, such as phosphoinositide 3-kinase (PI3K) (Harada et al., 2003; Pages et al., 1994), Lck (Holdorf et al., 1999; Liu et al., 2000), Grb2 (Raab et al., 1995), Gads (Watanabe et al., 2006), Itk, Vav (Villalba et al., 2000), PKB/Akt (Kane et al., 2001), PP2A (Alegre et al., 2001; Chuang et al., 2000), and PKCθ (Villalba et al., 2000), have been implicated in CD28-mediated co-stimulatory signals. However, since these molecules also function in TCR downstream signals, it is difficult to parse CD28-specific cascades qualitatively and quantitatively.

Immune responses are initiated by the communication between Ag-specific T cells and APCs for Ag recognition and T cell activation. An immunological synapse (IS) is formed at the T cell—APC interface and constituted by a c-SMAC containing TCR/CD3 complex and peripheral-SMAC (p-SMAC) containing LFA-1 (Grakoui et al., 1999; Monks et al., 1998). An IS was dynamically generated in the interface between T cells and B cells or a glass-supported planar bilayer, while a multifocal pattern of TCR, not a c-SMAC, was been observed between T cells and dendritic cells (DCs) (Brossard et al., 2005). We recently reported that T cell activation is spatiotemporally regulated by TCR MCs containing receptors, kinases, and adaptors (Campi et al., 2005; Saito and Yokosuka, 2006; Yokosuka et al., 2005). As the initial step of T cell activation, TCRs form small clusters at T cell—APC or —bilayer interface. Since these clusters contain both TCRs and phosphorylated proteins, and intracellular calcium levels are increased when a few MCs are generated, TCR MCs are supposed to function as signalsomes for T cell activation. As a subsequent step, only TCRs translocate to the center of the interface to result in c-SMAC formation. TCR MCs containing kinases and adaptors are observed only at the peripheral edge of T cells and not in c-SMAC. These findings mainly from planar bilayer system imply that TCR MCs are responsible for Ag recognition and the induction of activation signals both at initial contact and at later stage for maintenance of activation, and that c-SMAC are unable to sustain signaling (Varma et al., 2006). This concept of MCs serving as a key signalsome in T cell activation has raised important questions on how CD28-mediated co-stimulation is spatially and temporally regulated in the relationship with TCR MCs for the full activation of T cells.

CD28 was previously reported to traffic into the T cell—APC interface and co-localize with PKCθ upon Ag recognition (Egen and Allison, 2002; Pentcheva-Hoang et al., 2004). Furthermore, regarding the localization of CD28 in IS, CD28 was reported to be localized at c-SMAC (Bromley et al., 2001) or segregated from TCR in IS (Andres et al., 2004a; Huang et al., 2002; Tseng et al., 2005). Similar to TCR signals, CD28 signals were suggested to precede

c-SMAC formation, since CD28 upregulated TCR-induced intracellular calcium levels within seconds after T cell—APC conjugations. CD28 has also been implicated to localize in lipid rafts and augments the recruitment of TCR downstream molecules to lipid rafts. However, dynamic regulation of CD28 and its related signaling molecules have been poorly understood.

We report here the molecular imaging analysis on CD28-mediated co-stimulation that CD28 was recruited coordinately with TCR to MCs and then recruited PKCθ to TCR-CD28 MCs by associating together, resulting in the initial activation of T cells. Furthermore, CD28 plays a role in retaining PKCθ at a spatially unique and dynamic sub-zone of c-SMAC, leading to sustained signals for T cell activation.

Results

Cluster formation of CD28 at TCR MCs and c-SMACs

To examine the dynamic movement of CD28 on a live T cell, we visualized CD28 during T cell activation on a glass-supported planar bilayer by objective total internal reflection fluorescence microscopy (TIRFM) (Tokunaga et al., 1997). $CD4^+$ T cells from AND TCR-transgenic (AND-Tg) (specific for moth cytochrome *c* 88–103 ($MCC_{88–103}$) on I-E^k) CD28-deficient ($^{-/-}$) mice were introduced with EGFP-tagged CD28 (EGFP-CD28) by retroviral infection. These T cells were settled onto a planar bilayer containing glycophosphatidylinositol (GPI)-anchored I-E^k loaded with $MCC_{88–103}$, ICAM-1-, and CD80-GPI (I-E^k/ICAM-1/CD80) (Bromley et al., 2001; Grakoui et al., 1999), and movement of EGFP-CD28 in the entire process of T—bilayer contact was imaged. The densities of I-E^k, ICAM-1, and CD80 were adjusted to those of lipopolysaccharide (LPS)-stimulated B cells approximately 250, 100, and 60–120 molecules/μm^2, respectively (Fig. 1A).

Similar to the clustering of TCR/CD3 (Campi et al., 2005; Yokosuka et al., 2005), CD28 was found to generate clusters at cell—bilayer interface as soon as a T cell attached and the clusters increased in number during cell spreading. CD28 MC formation was completely dependent on the presence of CD80 (Fig. 2A and Movie S1, S2). After c-SMAC formation, CD28 MCs continued to be generated at the periphery of the cell—bilayer interface and accumulated in the central region (Fig. 2B and Movie S3, S4). Then, we examined whether CD28 MCs move similar to TCR MCs; co-localize initially with TCR MCs and later with c-SMAC (Fig. 2C). Surprisingly, CD28 MCs were completely co-localized with TCR MCs within the first few minutes of the contact (Fig. 2C). Average number of CD28 MC is 136 ± 39.4 in representative ten cells at 2 min. Almost all CD28 MCs (93.9 ± 7.4 %) were initially overlapped with CD3. After c-SMAC formation, a majority of CD28 was translocated to the center but, unexpectedly, segregated from TCR; high-density regions of CD28 ($CD28^{high}$) and CD3 ($CD3^{high}$) were segregated from each other, although $CD28^{high}$ contained dim CD3 staining ($CD3^{dim}$), and $CD3^{high}$ contained dim CD28 staining ($CD28^{dim}$) (Fig. 2C, D). Comparing to the c-SMAC observed in the absence of CD28—CD80 interaction, $CD3^{high}$ regions were formed as less massive clusters because $CD28^{high}$ interfered with the formation of such massive $CD3^{high}$ region. Collectively, $CD28^{high}$ appeared to be localized at relatively outer region of c-SMAC. We also utilized a planar bilayer containing Cy5-labeled ICAM-1-GPI as a marker for p-SMAC to investigate whether $CD28^{high}$ regions were localized in c- or p-SMACs. The ICAM-1 ring merged with LFA-1 and surrounded both $CD28^{high}$ and $CD28^{dim}$ regions, indicating that these CD28 clusters are localized in a previously unexplored outer region of c-SMAC (Fig. 2E). Collectively, these data show that CD28 is initially accumulated and localized at TCR MCs upon Ag-stimulation, and is later sorted to the outer region of c-SMAC as a novel compartment in IS.

Ligand-dependent but signal-independent formation of CD28 clusters

To examine whether particular downstream signals of CD28 are required for its MC formation, various EGFP-tagged various CD28 mutants were reconstituted into AND-Tg CD28$^{-/-}$ T cells. Each EGFP-CD28 contained a mutation in CD80/CD86-binding (Y123A), dimerization (C142S), or PI3K and Grb2/Gads-binding (Y189F), or a deletion of cytoplasmic 16 amino acids critical for lipid raft association (Δ16) or the entire cytoplasmic tail (ΔCP) (Andres et al., 2004b; Holdorf et al., 1999; Pages et al., 1994; Schneider et al., 1995). The surface expression levels of all CD28 mutants were nearly equal on activated T cells (data not shown). We found no significant differences in MC formation and distribution of CD28 both at initial contact and after c-SMAC formation among all CD28 mutants, except Y123A. Y123A failed to form CD28 MCs, whereas even CD28ΔCP mutant formed clusters (Fig. 3), indicating that CD28 MC formation depends on CD28—CD80 bindings but not on downstream signals through CD28. Nonetheless, the CD28 cytoplasmic domain may still recruit or associate with specific signaling molecules for co-stimulation.

CD28—CD80/CD86 binding has been shown to enhance both T cell proliferation and IL-2 production as co-stimulatory functions. Since we previously demonstrated that CD80-GPI enhances IL-2 production from naïve T cells on a planar bilayer (Bromley et al., 2001), we applied silica beads coated with the same I-E^{k}/ICAM-1/CD80-containing liposomes to stimulate T cells. AND-Tg naïve T cells showed marked increase in IL-2 production, proliferation, and CD69 expression upon bead stimulation (Fig. 1B-D). Similar results were obtained with effector T cells (Fig. S1).

CD28 clusters and its down stream signals

We analyzed a set of candidate molecules that move and co-localize with CD28 on a planar bilayer. TCR proximal signals were first analyzed by staining for phosphorylated CD3ζ (Fig. S2) or Zap70 (data not shown), but their phosphorylation status were not altered by the presence of CD80-GPI (Herndon et al., 2001). Then, we analyzed PI3K as a likely candidate for mediating co-stimulation, since PI3K was clearly demonstrated to bind ‘YMNM’ motif of CD28 cytoplasmic tail and to augment IL-2 production (Harada et al., 2003;Truitt et al., 1994). When AND-Tg T cells expressing EGFP-p55α as an indicator of type I PI3K were plated on an I-E^{k}/ICAM-1/CD80 planar bilayer, p55α clusters were transiently observed at the entire cell—bilayer interface. But they disappeared soon after moving toward the center and were not accumulated at c-SMAC similar to Zap70 and SLP-76 (Yokosuka et al., 2005) (Fig. S3A). The presence of CD80-GPI on a planar bilayer resulted in a slight but significant enhancement of size (0.050 ± 0.026 with CD80-GPI; 0.037 ± 0.024 without CD80-GPI) and fluorescence intensity of EGFP-p55α clusters (0.282 ± 0.160 with CD80-GPI; 0.182 ± 0.109 without CD80-GPI) (Fig. S4), confirming that PI3K is recruited to and enriched at TCR-CD28 MCs through CD28—CD80 bindings during initial activation. However, these movements of PI3K clusters did not simply correlate with the accumulation of CD28 at c-SMAC (Fig. S4). Two-color analysis of AND-TCR T cell hybridomas expressing both ECFP-CD28 and EYFP-p85α confirmed this result; initial colocalization of PI3K with TCR-CD28 clusters and the dissociation from CD28 in c-SMAC later (Fig. S3B). Catalytic subunit p110δ showed similar movement to p55α and p85α (data not shown). Furthermore, we analyzed cluster formation of Grb2, Gads, Vav1, and Itk in AND-Tg T cells expressing each EGFP fusion protein since these molecules have been suggested to functionally correlate with CD28 co-stimulation, however no accumulation at c-SMACs was observed, regardless of the presence of CD80-GPI (data not shown).

We then analyzed the movement of PKCθ using the foregoing assay, since PKCθ is activated after stimulation through both TCR and CD28 (Berg-Brown et al., 2004; Pfeifhofer et al., 2003; Sun et al., 2000), segregated in IS with CD28 co-stimulation, recruited to the lipid raft,

and plays a critical role in NF-κB activation. AND-Tg T cells expressing ECFP-CD28 and EYFP-PKCθ were conjugated with a DC cell line, DC-1, expressing I-E^k, ICAM-1, and transfected CD80, and the localization of CD28 and PKCθ was imaged. As previously reported (Huang et al., 2002), almost all T cells (96.6%, n=56) showed clear accumulation and co-localization of CD28 with PKCθ as patched clusters on a $MCC_{88–103}$-pulsed $CD80^+$ DC-1 (Fig. 4A–C). Importantly, a majority of T cells (81.7%) exhibiting conjugate formation with $CD80^-$ DC-1 showed PKCθ patch 2 min after conjugation, whereas only a minor population (1.6 %) showed 20 min later (Fig. 4C). These data suggest that Ag stimulation in the absence of CD80 induces transient translocation of PKCθ to the plasma membrane (Fig. 4A, row 3, Fig. 4B, top, and Fig. 4C, left), and that the CD28—CD80 interaction is required for the co-clustering of CD28 and PKCθ and for the stable and sustained translocation of PKCθ at the T cell—APC interface (Fig. 4A, B and Fig. 4C).

We further analyzed the kinetics and distribution of PKCθ using a planar bilayer and AND-Tg T cells expressing EGFP-PKCθ. PKCθ clusters were transiently observed even in the absence of CD80-GPI (Fig. 4D and Movie S5). In contrast, PKCθ accumulated to form clear clusters and persisted on the bilayer with CD80-GPI at initial activation (Fig. 4D and Movie S6). Furthermore, after c-SMAC formation, PKCθ clusters were accumulated at the central region of the cell—bilayer interface in an annular pattern, which lasted for at least 60 min (Fig. 4E and Movie S7, S8). These data demonstrated that CD28—CD80 interaction enhanced the accumulation of PKCθ both at MCs initially and at the central region of cell—bilayer interface after c-SMAC formation.

CD28-mediated recruitment of PKCθ to TCR MCs and c-SMACs

Next, we examined whether PKCθ clusters co-localized with TCR or CD28 during initial and sustained activation. Co-staining of PKCθ clusters with CD3 revealed that 95.2 % of PKCθ clusters merged with TCR MCs at initial contact (2 min, Fig. 5A). After c-SMAC formation (20 min), 76.5% of T cells showed PKCθ accumulated in $CD3^{dim}$ in an annular form and excluded from $CD3^{high}$ in c-SMAC (Fig. 5A, B). As this PKCθ accumulation resembles CD28 clusters, we examined the co-localization of CD28 with PKCθ using AND-Tg $CD28^{-/-}$ T cells expressing both EYFP-PKCθ and ECFP-CD28 on a planar bilayer. Depending on CD28—CD80 interaction, 93.4% of the cells initially exhibited co-localization of PKCθ with TCR-CD28 MCs (Fig. 5C, D). Thereafter, PKCθ was translocated to and accumulated at the center of the interface. After c-SMAC formation, PKCθ was persistently localized with CD28 at the outer region of c-SMAC by segregating from core CD3 (Fig. 5E, F). A majority of the cells with annular form of CD28 clusters (81.8 %) were co-localized with both PKCθ clusters and $CD3^{dim}$. As shown in Fig. 2E, annular form of PKCθ-CD28 clusters were settled in c-SMAC (Fig. 5G). PKCθ and CD28 clusters in an annular form were also imaged at the interface between AND-Tg T cells expressing EGFP-PKCθ and DC-1, though lower frequency and less clear images than a planar bilayer due to membrane ruffling (Fig. S5 and Movie S9).

To understand the mechanism of CD28-mediated PKCθ recruitment, we examined the physical association between CD28 and PKCθ. Indeed, we found that PKCθ was co-precipitated with CD28 in lysates from T cell hybridomas expressing both ECFP-CD28 and EYFP-PKCθ (the same cells for imaging in Fig. 4A, B) upon PMA stimulation (Fig. 5H, left four columns in PMA (−) and (+)). More importantly, this association was identified in both effector and naïve T cells from mice upon PMA stimulation (Fig. 5I and data not shown). The CD28—PKCθ assembly appears to be weak because the association was only detectable by using mild detergent such as digitonin (Fig. S6), these results suggest that CD28 recruits PKCθ by forming the assembly although there is no evidence yet for the direct interaction of CD28 and PKCθ.

5C.C7-Tg T cells, whose Ag-specificity is the same as AND-Tg T cells, generate smaller c-SMACs as they have a lower TCR affinity than AND-Tg T cells upon stimulation with the

same concentrations of Ag on a planar bilayer. Under the condition in which c-SMAC was not well-formed by 5C.C7-Tg T cells with lower concentrations of $MCC_{88–103}$ (1 and 0.1μM), PKCθ were still accumulated in an annular form (Fig. S7). This results suggest that annular accumulation of PKCθ clusters are generated without strong TCR—MHCp interactions which leads to clear c-SMAC formation, but dependently on the CD28—CD80 interaction.

Dynamic maintenance of CD28-PKCθ clusters at c-SMAC

The critical role of CD28 in retaining PKCθ at c-SMAC was confirmed by interrupting CD28—CD80 binding, using Ig fusion proteins of cytotoxic T lymphocyte antigen-4 (CTLA-4 WT Ig). The formation of both CD28 and PKCθ clusters in an annular form was diminished by the addition of CTLA-4 WT Ig but not CTLA-4 YA (Y139A) Ig, a binding mutant for CD80/CD86. The percentage of the cells forming annular CD28 and PKCθ clusters was reduced from 87.2 % to 32.4 % and from 42.3% to null, respectively (Fig. 6A, B). Severe reduction of IL-2 production was observed, if CD28—CD80 binding was blocked by CTLA-4 WT Ig at 2 min after stimulation, when only TCR-CD28-PKCθ-containing MCs were generated, as well as at 10 min after stimulation, when CD28-PKCθ annular clusters were set up (Fig. 6C). Since most PKCθ molecules were accumulated at CD28 clusters after c-SMAC formation, these results suggest that both initial MCs and an annular form of PKCθ clusters were correlated with T cell function.

To further analyze CD28 function in the recruitment of PKCθ to plasma membrane, we examined the re-localization of PKCθ at CD28 clusters. In our systems, CD28 MCs were generated and accumulated at the central region of the interface between T cells and I-E^k/ICAM-1/CD80 planar bilayers without $MCC_{88–103}$. PKCθ was mainly localized in cytosol without Ag stimulation, however it was efficiently translocated to CD28 clusters upon PMA stimulation (Fig. 6D, E). These results suggest that CD28 clusters recruit and retain PKCθ, and induce the formation of annular form of PKCθ clusters.

TCR clusters in c-SMAC were found to be relatively stable based on the fluorescence recovery after photobleaching (FRAP) study (Grakoui et al., 1999). We investigated the dynamics of the annular clusters of both CD28 and PKCθ in c-SMAC by FRAP (Fig. 6F, G and Movie S10, S11). Indeed, both CD28 and PKCθ showed rapid recovery of their clusters, indicating active maintenance of the structure and dynamic exchange within c-SMAC. PKCθ exhibited more rapid and complete recovery than CD28, probably due to its higher mobility as a cytoplasmic protein. These data suggest that the cytoplasmic tail of CD28 functions to dynamically recruit and concentrate PKCθ through assembly with them, and indicate that the annular formation of PKCθ clusters is dynamically generated and maintained by recruiting CD28-PKCθ from peripheral TCR-CD28 MCs.

Furthermore, PKCθ clusters in annular form were stained with anti-phospho-PKCθ Abs at the outer region of c-SMAC in a CD28—CD80 dependent manner in normal T cells, although a question on the specificityof the Ab has been raised (Lee et al., 2005) (Fig. S8), suggesting that PKCθ accumulated in the annular form of clusters was active to induce co-stimulatory signals.

Regulation of PKCθ translocation to TCR MCs by CD28 signals

To examine the requirement of the cytoplasmic tail of CD28 for PKCθ translocation to TCR-CD28 MCs, we established a series of AND-TCR T cell hybridomas expressing EYFP-PKCθ and various ECFP-CD28 mutants. First, we analyzed the translocation of PKCθ to the T cell—APC interface using DC-1 with or without CD80 expression (Fig. 7A, B). WT CD28 exhibited co-localization with PKCθ at T cell—APC interface upon Ag stimulation both 2 min and 30 min after conjugation. As in Fig. 3, PKCθ was translocated to membrane upon Ag

stimulation in T cells expressing CD28 with the mutated or deleted cytoplasmic tail (Y189F, Δ16, and ΔCP) membrane-translocation similar to WT CD28. In contrast, the cells exhibiting PKCθ patches co-localized with CD28 were decreased in number in these cells expressing CD28 tail was mutated or depleted (Y189F, Δ16, and ΔCP) 30 min after conjugation (Fig. 7B). The co-localization of CD28 with PKCθ was further analyzed on the planar bilayer using AND-Tg CD28$^{-/-}$ T cells (Fig. 7C) and AND-TCR T cell hybridomas (Fig. 7D, E). Whereas CD28 MCs were generated independently of cytoplasmic tail of CD28, PKCθ was not clearly recruited and formed MCs if the cytoplasmic tail was mutated or deleted (Fig. 3, Fig. 7C). These data demonstrated that CD28 cluster formation is independent of, but the recruitment of PKCθ to CD28 clusters is completely dependent on the cytoplasmic tail of CD28. Quantification of the number of AND-TCR T cell hybridomas exhibiting co-localization of clusters of PKCθ and CD28 WT or mutant clusters was shown in Fig. 7D and E. Consistent with these imaging data, biochemical analysis revealed that physical association between PKCθ and CD28 bearing cytoplasmic mutations were much weaker than those of WT CD28 (Fig. 5H). To clarify the function of the co-localization of CD28 with PKCθ within the same TCR MCs, AND-Tg T cells from CD28$^{-/-}$ mice were reconstituted with these CD28 mutants and stimulated with anti-CD28 Abs plus PMA to analyze co-stimulatory function (Fig. 7F). We found a strong correlation between the CD28—PKCθ co-localization, physical association and CD28-mediated co-stimulation, suggesting that CD28-mediated co-stimulation for the full activation of T cell is mediated by the recruitment of PKCθ to TCR-CD28 MCs.

Discussion

In this study, we illustrated the dynamic aspects of the mechanisms of CD28-mediated co-stimulation in relation to TCR MCs. CD28 is co-localized with TCR to form TCR-CD28 MCs together with signaling molecules as signalsomes, where CD28 plays a critical role in recruiting PKCθ to MCs at initial activation, and then to the outer region of c-SMAC possibly for sustained activation to exhibit effector functions. Previous studies have indicated that TCR MCs generated at the periphery of IS induce activation signals while c-SMAC may not be responsible for transducing activation signals, on the basis of our observation that phosphorylated proteins are localized almost in peripheral MCs and not obviously detected in c-SMAC (Yokosuka et al., 2005), and that Ca^{2+} signaling is not sustained in the absence of peripheral MCs (Varma et al., 2006). However, the present result of CD28-PKCθ signaling at the outer region of c-SMAC revises it to the idea that c-SMAC also provides signal competency for co-stimulation and that different signal clusters are responsible for TCR-mediated signals and co-stimulatory signals for the maintenance of T cell activation.

The translocation of CD28 to the T cell—APC interface before c-SMAC formation was previously reported (Andres et al., 2004a), but we demonstrated here the co-localization of CD28 with TCR and its downstream molecules as a TCR-CD28 MC using a planar bilayer system. This co-localization of TCR with CD28 in the same MC coincides with the findings that Lck phosphorylates both TCR and CD28 after TCR engagement, and that CD28 shares most of the downstream molecules with TCR. We searched for a signaling molecule contributing specifically to CD28 signals that initially co-localizes with TCR MCs and then translocates to CD28 clusters at the outer region of c-SMAC. We demonstrated that CD28 enhanced the co-localization of PI3K with CD28, but PI3K clusters were generated onlytransiently and did not accumulate at c-SMAC. We finally observed that PKCθ met the criteria for the specific mediator of CD28 signals; initial accumulation at TCR-CD28 MCs as well as at c-SMAC later.

PKCθ is widely known as a downstream molecule of CD28. PKCθ- and CD28-deficient animals demonstrated similar functional defects (Pfeifhofer et al., 2003; Sun et al., 2000), although the physical interaction has not been shown. We provided evidence of the functional

assembly between CD28 and PKCθ in three aspects. 1) PKCθ is contained within early activation signalsomes as TCR-CD28 MCs and translocated to c-SMAC with CD28. 2) Physical association of PKCθ with CD28 is demonstrated by co-immunoprecipitation upon PKCθ activation. 3)Functional importance of the early and later localization of PKCθ at TCR-CD28 MCs and at c-SMAC was evidenced in IL-2 production. Recently, CD19 was reported to enhance B cell functions through its co-localization with B cell receptors (BCRs) and Syk as BCR MCs (Depoil et al., 2008). These and our results suggest that MCs are initially generated as signalsomes with TCRs and BCRs and that their own co-stimulatory molecules are critical for the consequent signals.

In the last decade, PKCθ has been considered as a marker for c-SMAC during T cell activation (Monks et al., 1998), while CD28 was suggested to segregate PKCθ in IS (Huang et al., 2002; Tseng et al., 2005). In this study, in addition to the finding of co-localization of CD28-PKCθ in TCR-MC, we unveiled a new functional domain of c-SMAC by identification of a sub-region into which CD28 and PKCθ accumulated. The generation of this sub-region within cSMAC appears to depends on both localizations and densities of CD28 since PKCθ was co-localized with $CD28^{high}$ but not $TCR/CD3^{high}$. Furthermore, the formation of CD28 clusters is subjected to the density of CD28 and CD80/CD86 on T cells and APCs, respectively, and to the avidity of TCR to MHCp, substituting to the competition between CD28—CD80/CD86 and TCR—MHCp (unpublished observation). We propose here a functional region of c-SMAC, $CD3^{dim}$ $CD28^{high}$, as a co-stimulatory signalsome for T cell activation. We demonstrated that no signaling molecule was translocated to $CD3^{high}$, and that $CD3^{dim}$ was more flexible and dynamically regulated than $CD3^{high}$ by FRAP analysis (unpublished observation). Together with our previous report that lysobisphosphatidic acid (LBPA), a marker for protein degradation, was localized in c-SMAC (Varma et al., 2006), c-SMAC is suggested to be a negative regulatory compartment for T cell activation. The ratio of $CD3^{dim}$/$CD3^{high}$ appears to vary depending on the strength of TCR stimulation. A strong TCR stimulus may result inmore $CD3^{high}$ for endocytosis/degradation of TCR complexes, whereas a weak stimulus may result in more $CD3^{dim}$ that are susceptible to CD28-PKCθ-mediated co-stimulation. This is consistent with previous data suggesting the function of c-SMAC in negative regulation by signal strength-dependent TCR degradation (Cemerski et al., 2007). Our results suggest that c-SMACs may inherit ying and yang functions for the regulation of T cell activation: endocytosis/degradation of the TCR complex may mediate negative regulation through the $CD3^{high}$, whereas CD28-PKCθ accumulation could function for sustained T cell signaling through the spatially distinct region.

Our data depicted both spatial and temporal differences in the dynamics of PKCθ and Zap70/SLP-76 for MC formation. PKCθ may be recruited to the membrane toward diacylglycerol (DAG) or via phospholipase C-γ1 (PLCγ1)/DAG-independent manner (Villalba et al., 2002), and functionally activated by membrane translocation (Bi et al., 2001), while Zap70 and SLP-76 requires phosphorylation for the retention on cell surface by association with CD3 and LAT, respectively. Thus, PKCθ may associate with TCR-CD28 MCs via two steps—initial recruitment to the cell surface by DAG binding, followed by lateral movement to TCR-CD28 MCs through guidance by and/or association with CD28. Frequencies of cells with PKCθ translocation in CD28 Y189F, PI3K-bindingmutant, was lower than those in Δ16 mutant, in both T cell—APC and T cell—bilayer experiments (Fig. 7B, E), whereas stimulation of the Y189F CD28-expressing cells with PMA plus anti-CD28 Abs augmented the proliferation, suggesting that involvement of PI3K for the membrane translocation of PKCθ and that T cell response was partially rescued by PMA-mediated PKCθ relocation (Fig. 5H and Fig. 7F).

Several mechanisms could explain the CD28-mediated membrane translocation and co-localization with PKCθ. Both molecules might be recruited through lipid raft. It has been reported that CD28 engagement re-distributes lipid raft, and CD28 and PKCθ associate with

downstream molecules in lipid raft (Bi et al., 2001; Viola et al., 1999). However, we failed to observed cluster formation of a raft marker in our systems (data not shown). Alternatively, although PKCθ may be recruited through a DAG gradient generated at the T cell—APC interface (Spitaler et al., 2006), we have not observed gradient of a DAG marker (unpublished observation). Moreover, cell adhesion by CD28 may contribute to the functional recruitment of PKCθ to CD28 clusters through cytoskeletal rearrangement (Kaga et al., 1998). In this context, since filamin-A was reported to translocate into IS, associate with actin and PKCθ and enhanced IL-2 production in a CD28—CD80-dependent manner (Hayashi and Altman, 2006; Tavano et al., 2006), this mechanism might be involved in the co-localization of CD28 with PKCθ.

During T cell activation, the functional enhancement of T cell responses by CD28-mediated co-stimulation is prominent for T cell activation with weak TCR stimulus. Imaging studies have suggested that CD28 would support IL-2 production if no c-SMAC was generated (Purtic et al., 2005) or if APC carried a low concentration of Ag or self-Ag (Wulfing et al., 2002). In relation to these studies, we observed that CD28-PKCθ clusters could be generated even under the condition where c-SMAC is not clearly generated with lower affinity TCR, suggesting further differential regulation of two spatially distinct signaling clusters: peripheral MCs and annular clusters in c-SMAC may lead to the differential signaling pathways such as for Ca^{2+}/NFAT and NF-κB activation, respectively. The spatiotemporal regulation of TCR-CD28 cluster formation in c-SMAC may explain the complexity of intercommunicating molecules downstream of TCR and CD28.

At the outset of this study, we had strong evidence that TCR MCs generated initial and sustained signals and c-SMAC was primarily involved in signal termination. Whereas CD28 localization in IS had been extensively investigated, nano-scale imaging of co-stimulatory receptor CD28 and its signal transduction partners PI3K and PKCθ by TIRFM provided a new vision of two co-stimulatory mechanisms that are functionally critical: the early recruitment of PKCθ and PI3K to TCR-CD28 MCs and the late formation of a dynamic sub-region in c-SMAC enriched with PKCθ but depleted of TCR and PI3K.

Experimental Procedures

Reagents

Abs and reagents were purchased from the following suppliers: anti-mCD28, biotinylated anti-mCD3ε, FITC-anti-mCD11c, phycoerythrin (PE)-anti-mClass II, PE-mICMA-1, PE-anti-mCD69, PE-anti-mCD80, PE-anti-mCD86, and PE-isotype matched control Ig were from eBioscience; anti-PKCθ and anti-phospho PKCθ, from Santa Cruz; Alexa Fluor 647-anti-CD3 and Alexa Fluor 647-anti-phospho CD3ζ, from BD PharMingen; Alexa Fluor 488-streptoavidin, Alexa Fluor 647-anti-rabbit IgG, and Alexa Fluor 548-anti-hamster IgG from Molecular Probes; goat polyclonal anti-CD28 and rabbit polyclonal anti-PKCθ, from Santa Cruz; HRP-anti-GFP, from Miltenyi Biotec; and phorbol 12-myristate 13-acetate (PMA), from Sigma. Anti-mouse CD28 was provided by Dr. R. Abe (Science University of Tokyo, Japan).

Mice and cells

AND-Tg and 5C.C7-Tg mice on $Rag2^{-/-}$ background were provided by R. N. Germain (National Institutes of Health) and K. Yasutomo (Tokushima Univerity, Japan), respectively, and $CD28^{-/-}$ mice were purchased from Jackson Laboratories. The DC line, DC-1, was provided by J. Kaye. T cell hybridoma expressing AND-TCR was established by cell fusion of activated AND-Tg $CD4^{+}$ T cells with TCR-negative BW5147, as previously shown (See Current Protocols in Immunology).

Primary cell culture and transduction

Expression constructs were transiently transduced into Phoenix packaging cells (provided byDr. G. Norlan, Stanford University, CA), using LipofectAmine Plus (Invitrogen). Retroviral supernatants were concentrated tenfold by centrifugation at 8,000 *g* for 12 h. $CD4^+$ T cells were purified from AND-Tg $Rag2^{-/-}$ or AND-Tg $CD28^{-/-}$ $Rag2^{-/-}$ mice and stimulated with 5μM $MCC_{88–103}$ (ANERADLIAYLKQATK) and irradiated spleen cells from B10.BR mice. One day after stimulation, the cells were suspended in the retroviral supernatant and centrifuged at 1,000 *g* for 90 min in the presence of 8 μg/ml polybrene (Sigma) and 200 U/ml human recombinant interleukin 2 (Ajinomoto). At day 3 or later, 20–80% of T cells were transduced on the basis of the expression of EGFP, ECFP, or EYFP and sorted with FACSAria (BD) to obtain populations with homogenous fluorescence intensity. Cells were maintained for 5–14 d in RPMI1640 medium containing 10% FCS supplemented and recombinant IL-2.

Planar and spherical bilayers

GPI-anchored proteins of mouse I-E^k, ICAM-1, and CD80 were transfected into and purified from Chinese hamster ovary (CHO) or baby hamster kidney cells and were incorporated into dioleoyl phosphatidylcholine liposomes (DOPC, Avanti Polar Lipids). I-E^k- and ICAM-1-GPI were labeled with Cy5 mono NHS ester (Amersham Biosciences). Planar bilayers containing I-E^k-, ICAM-1-, and CD80-GPI were generated in a flow cell chamber system (Bioptechs). The expression levels of I-E^k, ICMA-1, and CD80 on the planar bilayer were quantified using silica beads 5μm in diameter (Bangs Laboratories). Silica beads were loaded with DOPC containing I-E^k-, ICMA-1-, and CD80-GPI in the same concentrations as that of planer bilayer, stained with FITC-labeled anti-I-E^k (14-4-4), anti-ICMA-1 (YN1/1), or anti-CD80 Abs (16.10A1), analyzed by FACSCalibur (BD). The densities of I-E^k, ICMA-1, and CD80 on a bilayer were calculated based on standard FITC beads (Bangs Laboratories) and adjusted to approximately 250, 100, and 60–120 molecules/μm^2, respectively. Planar bilayers were loaded with 10μM $MCC_{88–103}$ in citrate buffer, pH 4.5, for 24 h at 37 °C, blocked with 5% nonfat dried milk in PBS for 1 h at 37 °C, and left to stand in the assay medium. All experiments in planar bilayers were performed in HEPES-buffered saline containing 1% FCS, 2 mM $MgCl_2$, and 1 mM $CaCl_2$.

TIRF imaging

Cells were imaged with TIRFM as previously described (Tokunaga et al., 1997). A solid-state laser (488 nm, 20 mW; Sapphire 488-20-OPS, Coherent) and an inverted microscope (IX-81, Olympus, Japan) were used. Images were captured with an electron-bombarded charge-coupled device camera (C-7190-23; Hamamatsu Photonics).

Fluorescence imaging with planar bilayer

Cells transduced with various fluorescent-tagged proteins or stained by Fab Abs were real-time imaged by TIRF or confocal microscopy. For the immuno-fluorescent staining, the cells on a planar bilayer were fixed with 4% paraformaldehyde and stained with indicated Abs in 1% BSA PBS 0.3% Saponin for 30 min at 25 °C after blocking with 1% BSA PBS 0.3% Saponin. All images were collected on a Leica DMIRES2 system and data were analyzed with Leica confocal software.

T cell-APC conjugation assay

DC-1 cells were pre-pulsed overnight at 37 °C with 5μM MCC peptide and washed before assay. 2.5×10^4 AND-TCR T cell hybridomas expressing ECFP-CD28 and/or EYFP-PKCθ were cultured with DC-1 cells on glass bottom dish for real-time imaging or on 12 mm cover slips for fixing and staining.

T cell stimulation with silica beads

$CD4^+$ T cells were prepared from AND-Tg mice on $Rag2^{-/-}$ background by magnetic cell sorting (Miltenyi Biotec). $5–10 \times 10^4$ naïve or effector $CD4^+$ T cells were stimulated with silica beads coated with lipid bilayer containing I-E^k-, ICAM-1-, and CD80-GPI prepulsed with $MCC_{88–103}$ in a 96-well round-bottomed dish. At 6 h after stimulation, cells were stained with anti-CD69 Abs and analyzed by FACSCalibur. At 48 h, IL-2 in supernatants was measured by ELISA. Also at 48 h, the cells were pulsed with 2 Ci/well of ^{3}H-thymidine for 12 h and the incorporated radioactivity was measured with a Microbeta scintillation counter (Amersham Pharmacia Biotech).

Supplementary Material

Refer to Web version on PubMed Central for supplementary material.

Acknowledgments

We would like to thank Dr. R. Verma for discussion, Drs. J. P. Allison and R. Abe for reagents, Drs. R. N. Germain for mice, and Ms. H. Yamaguchi and S. Kato for secretarial assistance. We especially thank the late Mrs. T. Starr for instructing the planar bilayer preparation. This work was supported by a Grant-in-Aid for Priority Area Research from the Ministry of Education, Culture, Sports, Science and Technology of Japan (T. Y., A. H. T., M. T. and T. S.), New Energy Development Organization (M. T.), and the National Institutes of Health (AI043542 and AI044931 to M. L. D.).

References

Acuto O, Michel F. CD28-mediated co-stimulation: a quantitative support for TCR signalling. Nat Rev Immunol 2003;3:939–951. [PubMed: 14647476]

Alegre ML, Frauwirth KA, Thompson CB. T-cell regulation by CD28 and CTLA-4. Nat Rev Immunol 2001;1:220–228. [PubMed: 11905831]

Andres PG, Howland KC, Dresnek D, Edmondson S, Abbas AK, Krummel MF. CD28 signals in the immature immunological synapse. J Immunol 2004a;172:5880–5886. [PubMed: 15128767]

Andres PG, Howland KC, Nirula A, Kane LP, Barron L, Dresnek D, Sadra A, Imboden J, Weiss A, Abbas AK. Distinct regions in the CD28 cytoplasmic domain are required for T helper type 2 differentiation. Nat Immunol 2004b;5:435–442. [PubMed: 15004555]

Berg-Brown NN, Gronski MA, Jones RG, Elford AR, Deenick EK, Odermatt B, Littman DR, Ohashi PS. PKCtheta signals activation versus tolerance in vivo. J Exp Med 2004;199:743–752. [PubMed: 15024044]

Bi K, Tanaka Y, Coudronniere N, Sugie K, Hong S, van Stipdonk MJ, Altman A. Antigen-induced translocation of PKC-theta to membrane rafts is required for T cell activation. Nat Immunol 2001;2:556–563. [PubMed: 11376344]

Bromley SK, Iaboni A, Davis SJ, Whitty A, Green JM, Shaw AS, Weiss A, Dustin ML. The immunological synapse and CD28-CD80 interactions. Nat Immunol 2001;2:1159–1166. [PubMed: 11713465]

Brossard C, Feuillet V, Schmitt A, Randriamampita C, Romao M, Raposo G, Trautmann A. Multifocal structure of the T cell - dendritic cell synapse. Eur J Immunol 2005;35:1741–1753. [PubMed: 15909310]

Campi G, Varma R, Dustin ML. Actin and agonist MHC-peptide complex-dependent T cell receptor microclusters as scaffolds for signaling. J Exp Med 2005;202:1031–1036. [PubMed: 16216891]

Cemerski S, Das J, Locasale J, Arnold P, Giurisato E, Markiewicz MA, Fremont D, Allen PM, Chakraborty AK, Shaw AS. The stimulatory potency of T cell antigens is influenced by the formation of the immunological synapse. Immunity 2007;26:345–355. [PubMed: 17346997]

Chambers CA, Kuhns MS, Egen JG, Allison JP. CTLA-4-mediated inhibition in regulation of T cell responses: mechanisms and manipulation in tumor immunotherapy. Annu Rev Immunol 2001;19:565–594. [PubMed: 11244047]

Chuang E, Fisher TS, Morgan RW, Robbins MD, Duerr JM, Vander Heiden MG, Gardner JP, Hambor JE, Neveu MJ, Thompson CB. The CD28 and CTLA-4 receptors associate with the serine/threonine phosphatase PP2A. Immunity 2000;13:313–322. [PubMed: 11021529]

Depoil D, Fleire S, Treanor BL, Weber M, Harwood NE, Marchbank KL, Tybulewicz VL, Batista FD. CD19 is essential for B cell activation by promoting B cell receptor-antigen microcluster formation in response to membrane-bound ligand. Nat Immunol 2008;9:63–72. [PubMed: 18059271]

Egen JG, Allison JP. Cytotoxic T lymphocyte antigen-4 accumulation in the immunological synapse is regulated by TCR signal strength. Immunity 2002;16:23–35. [PubMed: 11825563]

Grakoui A, Bromley SK, Sumen C, Davis MM, Shaw AS, Allen PM, Dustin ML. The immunological synapse: a molecular machine controlling T cell activation. Science 1999;285:221–227. [PubMed: 10398592]

Harada Y, Ohgai D, Watanabe R, Okano K, Koiwai O, Tanabe K, Toma H, Altman A, Abe R. A single amino acid alteration in cytoplasmic domain determines IL-2 promoter activation by ligation of CD28 but not inducible costimulator (ICOS). J Exp Med 2003;197:257–262. [PubMed: 12538664]

Hayashi K, Altman A. Filamin A is required for T cell activation mediated by protein kinase C-theta. J Immunol 2006;177:1721–1728. [PubMed: 16849481]

Herndon TM, Shan XC, Tsokos GC, Wange RL. ZAP-70 and SLP-76 regulate protein kinase C-theta and NF-kappa B activation in response to engagement of CD3 and CD28. J Immunol 2001;166:5654–5664. [PubMed: 11313406]

Holdorf AD, Green JM, Levin SD, Denny MF, Straus DB, Link V, Changelian PS, Allen PM, Shaw AS. Proline residues in CD28 and the Src homology (SH)3 domain of Lck are required for T cell costimulation. J Exp Med 1999;190:375–384. [PubMed: 10430626]

Huang J, Lo PF, Zal T, Gascoigne NR, Smith BA, Levin SD, Grey HM. CD28 plays a critical role in the segregation of PKC theta within the immunologic synapse. Proc Natl Acad Sci U S A 2002;99:9369–9373. [PubMed: 12077322]

Kaga S, Ragg S, Rogers KA, Ochi A. Stimulation of CD28 with B7–2 promotes focal adhesion-like cell contacts where Rho family small G proteins accumulate in T cells. J Immunol 1998;160:24–27. [PubMed: 9551951]

Kane LP, Andres PG, Howland KC, Abbas AK, Weiss A. Akt provides the CD28 costimulatory signal for up-regulation of IL-2 and IFN-gamma but not TH2 cytokines. Nat Immunol 2001;2:37–44. [PubMed: 11135576]

Lee KY, D'Acquisto F, Hayden MS, Shim JH, Ghosh S. PDK1 nucleates T cell receptor-induced signaling complex for NF-kappaB activation. Science 2005;308:114–118. [PubMed: 15802604]

Liu Y, Witte S, Liu YC, Doyle M, Elly C, Altman A. Regulation of protein kinase Ctheta function during T cell activation by Lck-mediated tyrosine phosphorylation. J Biol Chem 2000;275:3603–3609. [PubMed: 10652356]

Monks CR, Freiberg BA, Kupfer H, Sciaky N, Kupfer A. Three-dimensional segregation of supramolecular activation clusters in T cells. Nature 1998;395:82–86. [PubMed: 9738502]

Pages F, Ragueneau M, Rottapel R, Truneh A, Nunes J, Imbert J, Olive D. Binding of phosphatidylinositol-3-OH kinase to CD28 is required for T-cell signalling. Nature 1994;369:327–329. [PubMed: 8183372]

Pentcheva-Hoang T, Egen JG, Wojnoonski K, Allison JP. B7–1 and B7–2 selectively recruit CTLA-4 and CD28 to the immunological synapse. Immunity 2004;21:401–413. [PubMed: 15357951]

Pfeifhofer C, Kofler K, Gruber T, Tabrizi NG, Lutz C, Maly K, Leitges M, Baier G. Protein kinase C theta affects Ca2+ mobilization and NFAT cell activation in primary mouse T cells. J Exp Med 2003;197:1525–1535. [PubMed: 12782715]

Purtic B, Pitcher LA, van Oers NS, Wulfing C. T cell receptor (TCR) clustering in the immunological synapse integrates TCR and costimulatory signaling in selected T cells. Proc Natl Acad Sci U S A 2005;102:2904–2909. [PubMed: 15703298]

Raab M, Cai YC, Bunnell SC, Heyeck SD, Berg LJ, Rudd CE. p56Lck and p59Fyn regulate CD28 binding to phosphatidylinositol 3-kinase, growth factor receptor-bound protein GRB-2, and T cell-specific protein-tyrosine kinase ITK: implications for T-cell costimulation. Proc Natl Acad Sci U S A 1995;92:8891–8895. [PubMed: 7568038]

Riley JL, June CH. The CD28 family: a T-cell rheostat for therapeutic control of T-cell activation. Blood 2005;105:13–21. [PubMed: 15353480]

Rudd CE, Schneider H. Unifying concepts in CD28, ICOS and CTLA4 co-receptor signalling. Nat Rev Immunol 2003;3:544–556. [PubMed: 12876557]

Saito T, Yokosuka T. Immunological synapse and microclusters: the site for recognition and activation of T cells. Curr Opin Immunol 2006;18:305–313. [PubMed: 16616469]

Salomon B, Bluestone JA. Complexities of CD28/B7: CTLA-4 costimulatory pathways in autoimmunity and transplantation. Annu Rev Immunol 2001;19:225–252. [PubMed: 11244036]

Schneider H, Cai YC, Prasad KV, Shoelson SE, Rudd CE. T cell antigen CD28 binds to the GRB-2/SOS complex, regulators of p21ras. Eur J Immunol 1995;25:1044–1050. [PubMed: 7737275]

Sharpe AH, Freeman GJ. The B7-CD28 superfamily. Nat Rev Immunol 2002;2:116–126. [PubMed: 11910893]

Spitaler M, Emslie E, Wood CD, Cantrell D. Diacylglycerol and protein kinase D localization during T lymphocyte activation. Immunity 2006;24:535–546. [PubMed: 16713972]

Sun Z, Arendt CW, Ellmeier W, Schaeffer EM, Sunshine MJ, Gandhi L, Annes J, Petrzilka D, Kupfer A, Schwartzberg PL, Littman DR. PKC-theta is required for TCR-induced NF-kappaB activation in mature but not immature T lymphocytes. Nature 2000;404:402–407. [PubMed: 10746729]

Tavano R, Contento RL, Baranda SJ, Soligo M, Tuosto L, Manes S, Viola A. CD28 interaction with filamin-A controls lipid raft accumulation at the T-cell immunological synapse. Nat Cell Biol 2006;8:1270–1276. [PubMed: 17060905]

Tokunaga M, Kitamura K, Saito K, Iwane AH, Yanagida T. Single molecule imaging of fluorophores and enzymatic reactions achieved by objective-type total internal reflection fluorescence microscopy. Biochem Biophys Res Commun 1997;235:47–53. [PubMed: 9196033]

Truitt KE, Hicks CM, Imboden JB. Stimulation of CD28 triggers an association between CD28 and phosphatidylinositol 3-kinase in Jurkat T cells. J Exp Med 1994;179:1071–1076. [PubMed: 7509360]

Tseng SY, Liu M, Dustin ML. CD80 cytoplasmic domain controls localization of CD28, CTLA-4, and protein kinase Ctheta in the immunological synapse. J Immunol 2005;175:7829–7836. [PubMed: 16339518]

Varma R, Campi G, Yokosuka T, Saito T, Dustin ML. T cell receptor-proximal signals are sustained in peripheral microclusters and terminated in the central supramolecular activation cluster. Immunity 2006;25:117–127. [PubMed: 16860761]

Villalba M, Bi K, Hu J, Altman Y, Bushway P, Reits E, Neefjes J, Baier G, Abraham RT, Altman A. Translocation of PKC[theta] in T cells is mediated by a nonconventional, PI3-K- and Vav-dependent pathway, but does not absolutely require phospholipase C. J Cell Biol 2002;157:253–263. [PubMed: 11956228]

Villalba M, Coudronniere N, Deckert M, Teixeiro E, Mas P, Altman A. A novel functional interaction between Vav and PKCtheta is required for TCR-induced T cell activation. Immunity 2000;12:151–160. [PubMed: 10714681]

Viola A, Schroeder S, Sakakibara Y, Lanzavecchia A. T lymphocyte costimulation mediated by reorganization of membrane microdomains. Science 1999;283:680–682. [PubMed: 9924026]

Watanabe R, Harada Y, Takeda K, Takahashi J, Ohnuki K, Ogawa S, Ohgai D, Kaibara N, Koiwai O, Tanabe K, et al. Grb2 and Gads exhibit different interactions with CD28 and play distinct roles in CD28-mediated costimulation. J Immunol 2006;177:1085–1091. [PubMed: 16818765]

Wulfing C, Sumen C, Sjaastad MD, Wu LC, Dustin ML, Davis MM. Costimulation and endogenous MHC ligands contribute to T cell recognition. Nat Immunol 2002;3:42–47. [PubMed: 11731799]

Yokosuka T, Sakata-Sogawa K, Kobayashi W, Hiroshima M, Hashimoto-Tane A, Tokunaga M, Dustin ML, Saito T. Newly generated T cell receptor microclusters initiate and sustain T cell activation by recruitment of Zap70 and SLP-76. Nat Immunol 2005;6:1253–1262. [PubMed: 16273097]

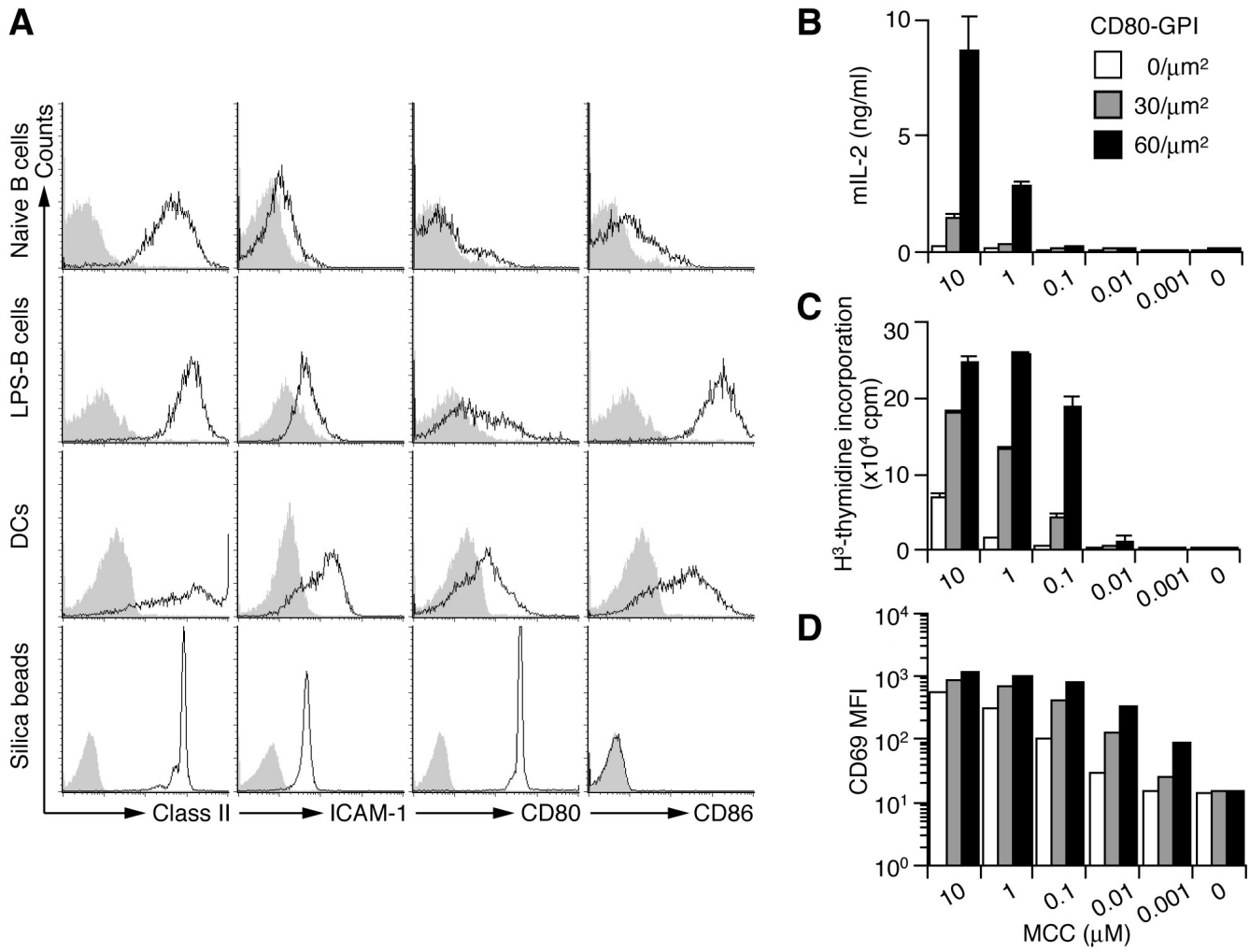

Figure 1.

Co-stimulatory function of CD80-GPI on lipid bilayers. (**A**) 5 μm silica beads were coated with lipid bilayer containing I-E^k, ICAM-1, and CD80 at the same ratio as that for planar bilayers. Naive and LPS-stimulated B cells, DCs, and silica beads were stained with Abs for Class II, ICAM-1, CD80, or CD86 and analyzed by FACS. (**B**-**D**) Naïve CD4$^+$ T cells from AND-Tg mice were stimulated with silica beads that were coated with lipid bilayer containing I-E^k, ICAM-1, and CD80 at various densities and were prepulsed with indicated doses of $MCC_{88–104}$. IL-2 production was measured by ELISA at 48 h (**B**), proliferation by ^{3}H-thymidine uptake at 60 h (**C**), and CD69 expression by FACS at 6 h after stimulation (**D**).

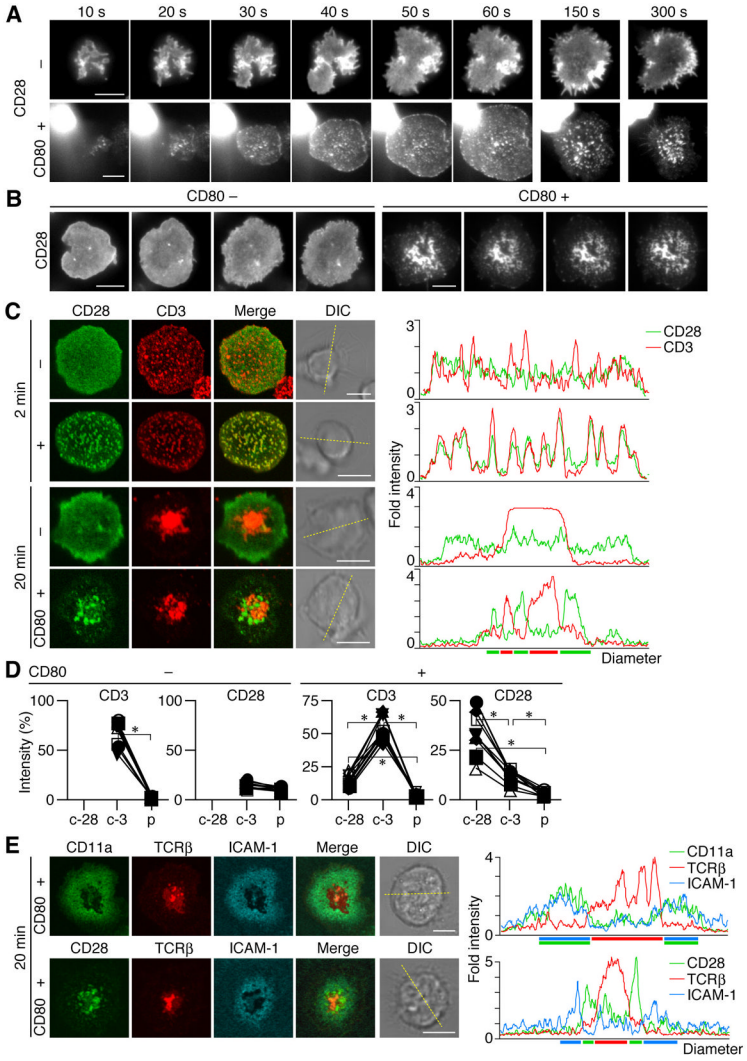

Figure 2.

Ligand-dependent clustering of CD28 at TCR/CD3 MCs and at c-SMAC. (**A**, **B**) AND-Tg T cells expressing EGFP-CD28 were plated on a planar bilayer containing I-E^k and ICAM-1 (top) plus CD80 (bottom) (prepulsed with $MCC_{88–104}$). Cells were imaged at video rate (30 frames/s) using TIRFM (time shown above images). Images from 10 s to 5 min are depicted in (**A**) and at 10 min after initial contact in (**B**), interval between images is 10 s. Real-time images in (**A**, **B**) are available in Movie S1-S4. (**C**) Cells in (**A**, **B**) were fixed at 2 or 20 min after cell—bilayer contact, stained for CD3, and imaged by confocal microscopy. Histograms on right panels show fold fluorescence intensities of EGFP-CD28 (green) and CD3 (red) on the diagonal yellow lines in DIC images. (**D**) Fluorescence intensities of CD3 and EGFP-CD28 in CD28 (c-28) or CD3 clusters (c-3) in c-SMAC or p-SMAC (p) were compared to the intensities of entire interfaces in the cells in (**C**) (20 min, bottom two rows) (n=10). Asterisk, p-value <0.001. (**E**) AND-Tg T cells expressing EGFP-CD11a (top) or EGFP-CD28 (bottom) were stained with Alexa Fluor 546-labeled anti-TCRβ Abs Fab and were plated on a planar bilayer containing I-E^k, CD80, and Cy5-labeled ICAM-1 (prepulsed with $MCC_{88–104}$). Cells were imaged real-time by confocal microscopy 20 min after contacts. Histograms on the right panels are shown as in (**C**). Scale bars, 5μm.

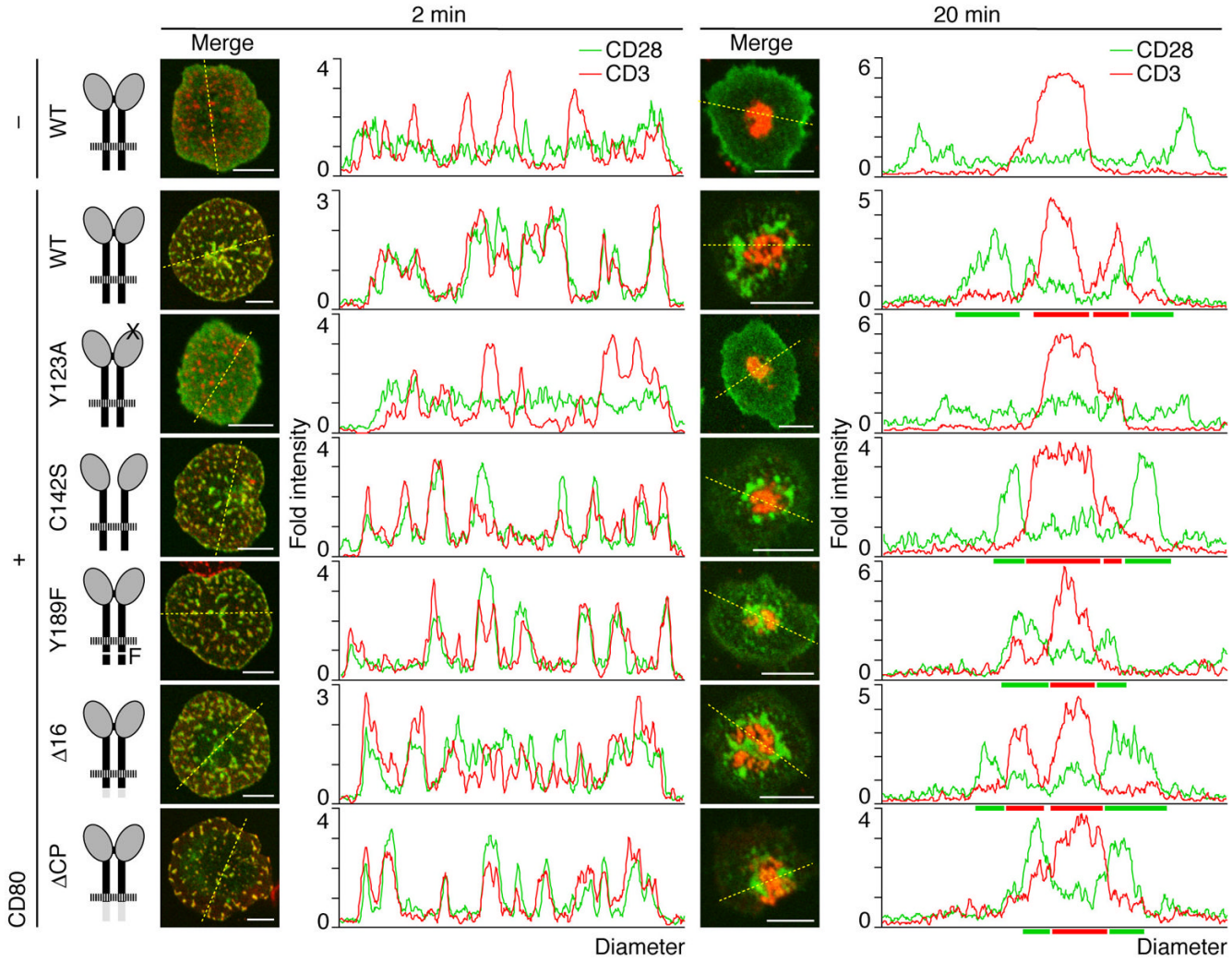

Figure 3.

CD28 cluster formation is independent of CD28 cytoplasmic tail. AND-Tg T cells from $CD28^{-/-}$ mice were reconstituted with EGFP-WT CD28 (top two rows) or various CD28 mutants (bottom five rows, Y123A, C142S, Y189F, Δ16, and ΔCP) by retroviral infection. Cells were plated on a planar bilayer containing $I\text{-}E^{k}$ and ICAM-1 (top row) plus CD80 (bottom six rows) (prepulsed with $MCC_{88–104}$), fixed 2 min (left columns) or 20 min after contact (right columns), and stained for CD3. The localizations of CD28 (green) and CD3 (red) were imaged by confocal microscopy and the fold fluorescence intensities on diagonal yellow lines were presented by histograms. Scale bars, 5μm.

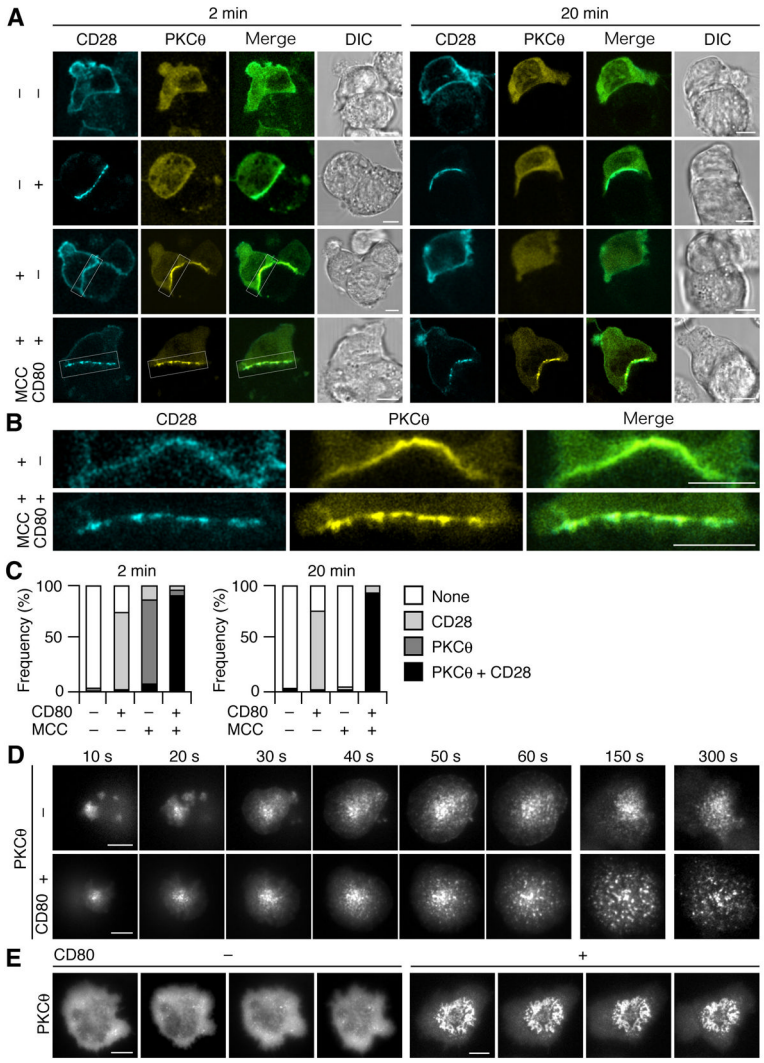

Figure 4.

CD28–CD80 binding maintains translocation of PKCθ to cell—cell and cell—bilayer interface. (**A**, **B**) AND-TCR T cell hybridomas expressing ECFP-CD28 and EYFP-PKCθ were conjugated with $MCC_{88–104}$-pulsed or unpulsed DC-1, expressing or not expressing CD80, and imaged by confocal microcopy 2 min or 20 min after conjugation. Magnified images of white squares in (**A**) are depicted in (**B**). (**C**) Conjugated pairs in (**A**) were categorized by translocation of ECFP-CD28 and/or EYFP-PKCθ at the interface (2 min, n=32, 108, 83, and 56; 20 min, n=70, 63, 62, and 44, from left to right). (**D**, **E**) AND-Tg T cells expressing EGFP-PKCθ were plated on a planar bilayer containing I-E^k and ICAM-1 (top) plus CD80 (bottom) (prepulsed with $MCC_{88–104}$). Cells were imaged at video rate (30 frames/s) using TIRFM (time shown above images). Images from 10 s to 5 min are depicted in (**D**) and at 10 min after initial contact in (**E**), interval between images is 10 s. Real-time images in (**D**, **E**) are available in Movie S5-S8. Scale bars, 5μm.

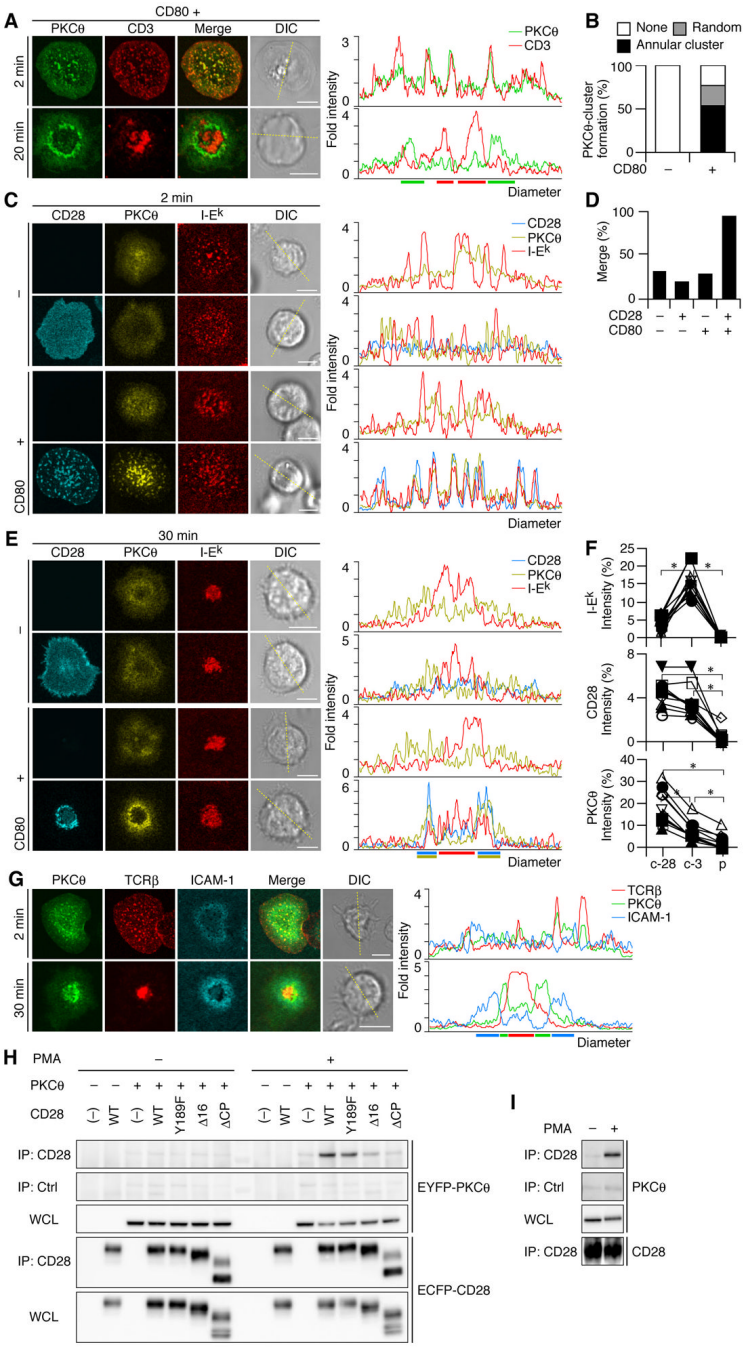

Figure 5.

PKCθ co-localizes with CD28 at TCR/CD3 MCs at initiation and forms annular clusters with CD28 after c-SMAC formation. (**A**, **B**) AND-Tg T cells expressing EGFP-PKCθ were plated on a planar bilayer containing I-E^k, ICAM-1, and CD80 (prepulsed with MCC$_{88–104}$), fixed at the indicated time, and stained for CD3. PKCθ clusters at 20 min (**A**, bottom) were categorized into random or annular clusters (**B**, CD80-, n=85; CD80+, n=132). (**C**-**E**) AND-Tg T cells from CD28$^{-/-}$ mice were introduce by EYFP-PKCθ (rows 1 and 3) plus ECFP-CD28 (rows 2 and 4) and plated on a planar bilayer containing Cy5-labeled I-E^k and ICAM-1 (top two rows) plus CD80 (bottom two rows). Cells were imaged by confocal microscopy 2 min after contact. (**D**) Percentage of cells containing I-E^k clusters co-localizing with PKCθ clusters in (**C**) (n=30,

16, 34, and 61, from left to right). (**E**, **F**) Co-localization of CD28, PKCθ, and I-E^k at c-SMAC was analyzed 30 min after cell—bilayer contact in (**C**). Fluorescence intensities of Cy5-I-E^k (top), ECFP-CD28 (middle), and EYFP-PKCθ (bottom) in CD28 (c-28) or CD3 clusters (c-3) in c-SMAC or p-SMAC (p) in (**E**, bottom row) were compared to the intensities of entire cell—bilayer interfaces (**F**, n=10). Asterisk, p-value <0.001. (**G**) AND-Tg T cells expressing EGFP-PKCθ were stained with Alexa Fluor 546-anti-TCRβ Abs Fab and plated on a planar bilayer containing I-E^k, CD80, and Cy5-labeled ICAM-1. Cells were imaged by confocal microscopy 2 min (top) or 30 min after contact (bottom). Histograms in (**A**, **C**, **E**, and **G**) are fold fluorescence intensities of indicated molecules on the diagonal yellow line in each DIC image. Scale bars, 5μm. (**H**, **I**) Physical interaction between CD28 and PKCθ upon activation in T cell hybridomas (**H**) and normal splenic T cells (**I**). AND-TCR T cell hybridomas expressing EYFP-PKCθ and ECFP-WT or cytoplasmic mutant CD28 in Fig. 3 were unstimulated (left) or stimulated for 2 min with 50 nM PMA (right). Cell lysates were immunoprecipitated with anti-CD28 (rows1 and 4) or control Abs (row 2), and blotted for EYFP-PKCθ (top three rows) and ECFP-CD28 (bottom two rows) (**H**). Splenic T cells were unstimulated (left) or stimulated (right) as in (**I**). Cell lysates were immunoprecipitated with anti-CD28 (rows 1 and 4) or control Abs (row 2) and blotted with anti-PKCθ (top three rows) or anti-CD28 Abs (bottom). WCL: whole cell lysate.

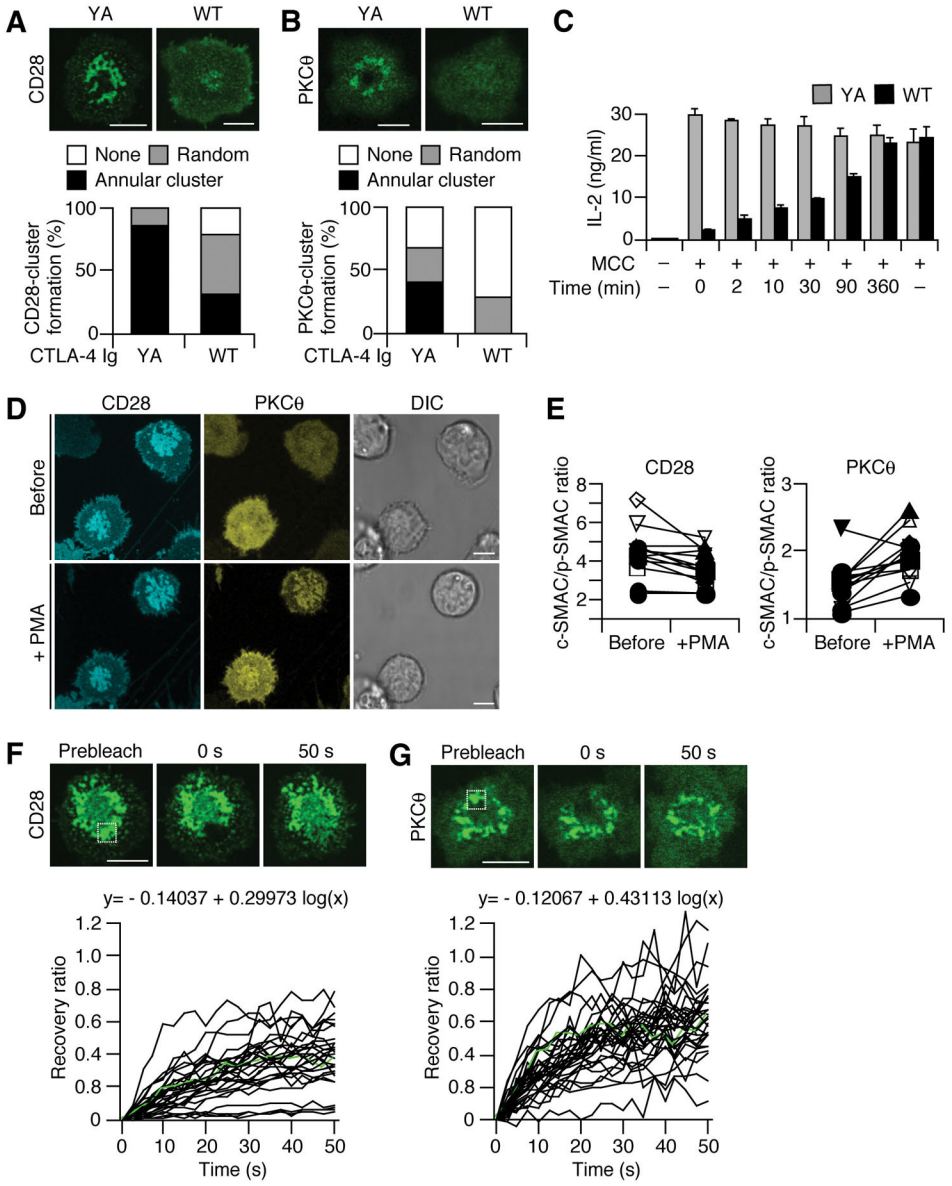

Figure 6.

Dynamic regulation of CD28-PKCθ clusters in an annular form at c-SMAC and their function in IL-2 production. (**A**, **B**) 5C.C7-Tg T cells expressing EGFP-CD28 (**A**) or EGFP-PKCθ (**B**) were plated on a planar bilayer containing I-E^k, ICAM-1, and CD80 (prepulsed with $MCC_{88–104}$) for 20 min and further incubated with CTLA-4 WT or Y139A Ig for 10 min. Cells were imaged by confocal microscopy (top) and categorized into random or annular clusters (bottom) (CD28 YA, n=141; WT, n=114; PKCθ YA, n=52; WT, n=44). (**C**) Reduction of IL-2 production by blocking of CD28—CD80 interaction. 5C.C7-Tg effector T cells were stimulated by splenic B cells pulsed or unpulsed with $MCC_{88–104}$, and added by CTLA-4 WT (black) or Y139A Ig fusion proteins (gray) at the indicated times. After two days, IL-2 was measured by ELISA. (**D**, **E**) Re-localization of PKCθ to CD28 clusters. AND-TCR T cell hybridomas expressing both ECFP-CD28 and EYFP-PKCθ were plated on a planar bilayer containing I-E^k, ICAM-1, and CD80 without $MCC_{88–104}$, and allowed to develop CD28 clusters for 15 min. Translocation of EYFP-PKCθ in the same cells was imaged before and

after 5 μM PMA stimulation (**D**). The average intensities of ECFP-CD28 (left) and EYFP-PKCθ (right) in c-SMAC in the cells in **D** were compared to those of the entire interfaces (**E**, n=11). (**F**, **G**) Dynamism of CD28 and PKCθ clusters in an annular form. AND-Tg T cells expressing EGFP-CD28 (**F**) or EGFP-PKCθ (**G**) were plated on a planar bilayer as in (**A**) for 20 min. Recoveries of CD28 and PKCθ were analyzed by FRAP at specific regions (white square) of the annular clusters. Images were obtained every 2.5 s by confocal microscopy and the fluorescence recovery ratios were calculated (**F**, n=28; **G**, n=30). Green lines in graphs depict the recovery ratios of cells in top panels. Mathematical formulas are approximated curves involving 28 or 30 cells. Real-time images in (**F**, **G**) are available in Movie S9 and S10. Scale bars, 5μm.

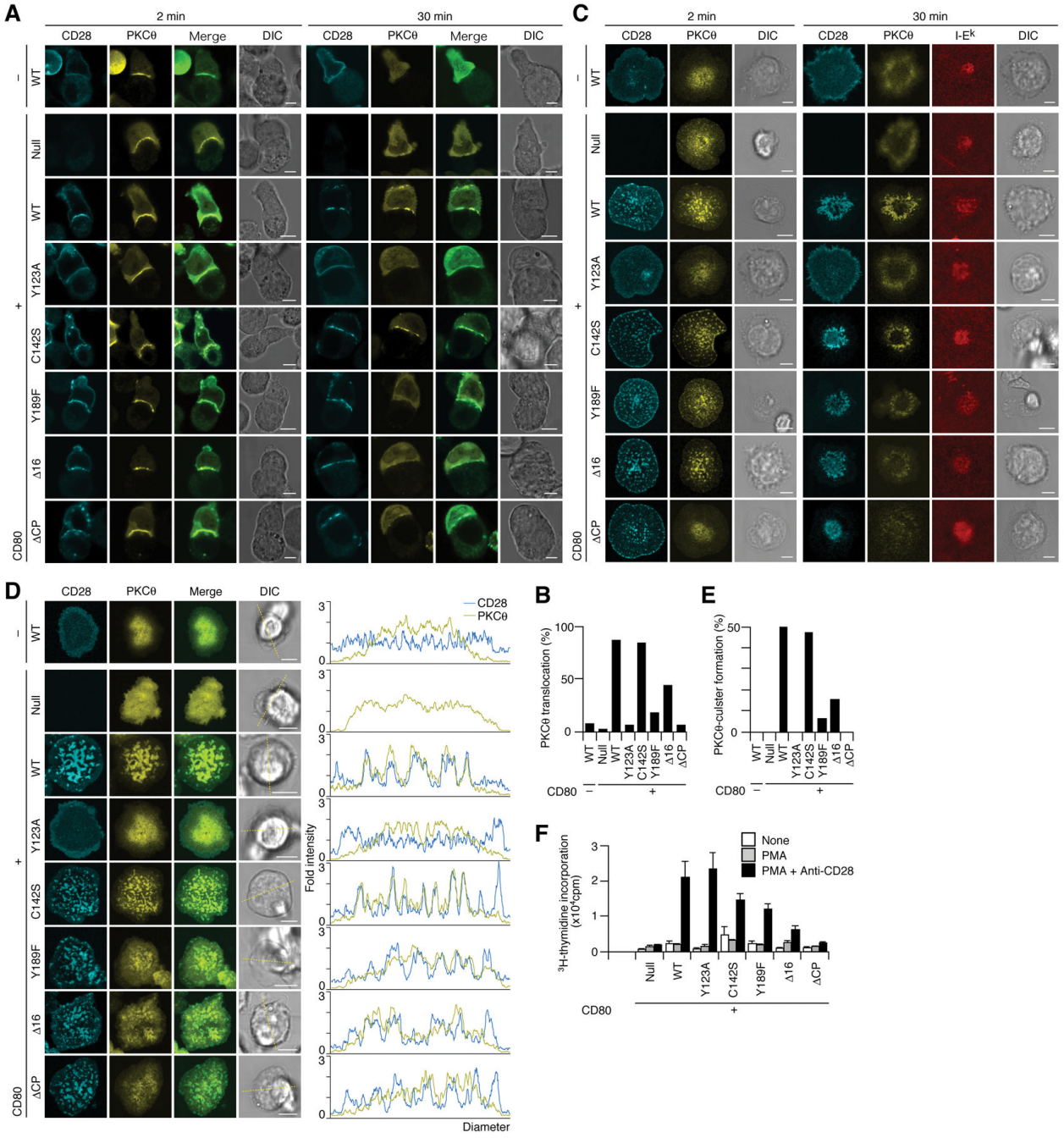

Figure 7.

Functionof CD28 cytoplasmic tail in the translocation of PKCθ to T cell—APC interface and TCR-CD28 MCs. (**A**, **B**) AND-TCR T cell hybridomas expressing EYFP-PKCθ and ECFP-WT or mutant CD28 were conjugated with $MCC_{88–104}$-pulsed DC-1 cells without (topmost row, −) or with (bottom seven rows, +) CD80. Cells were imaged real-time at the indicated time by confocal microscopy (ECFP-CD28, cyan; EYFP-PKCθ, yellow). In fixed samples, conjugating pairs with PKCθ translocated to cell cell interface were counted in (**B**, n=60, 68, 60, 115, 68, 65, 73, and 122 from left to right). (**C**) AND-Tg T cells from $CD28^{-/-}$ mice were reconstituted with ECFP-WT or various mutant CD28 (cyan) and EYFP-PKCθ (yellow), plated on a planar bilayer containing Cy5-I-E^k (red) and ICAM-1 plus CD80 (prepulsed with

$MCC_{88–104}$), and imaged by confocal microcopy in real-time 2 min or 30 min after cell—bilayer contacts. (**D**, **E**) AND-TCR T cell hybridomas in **A** were plated on a planar bilayer as in (**C**). Images were obtained in real-time by confocal microscopy immediately after contact. Histograms show fold fluorescence intensities of ECFP-CD28 (blue) and EYFP-PKCθ (yellow) on the diagonal yellow lines in DIC images. Percentages of cells containing PKCθ clusters in (**D**) are calculated in (**E**, n=38, 26, 70, 42, 70, 83, 59, and 44 from left to right). (**F**) AND-Tg T cells from $CD28^{-/-}$ mice were reconstituted with WT or various mutant CD28 and stimulated with PMA in combination with anti-CD28 Abs. T cell proliferation was measured 48 h after stimulation. Scale bars, 5μm.